CORROSION SCIENCE AND TECHNOLOGY, Vol.2, No.3(2003), pp.109~116

The Relationship Between Hydrogen Trapping Behavior and SSCC Suceptibility of API X60/65 Grade Steels

Jae Myung Lee, Jin Suk Kim, and Kyoo Young Kim

Pohang University of Science and Technology
Center for Advanced Aerospace Materials Pohang 790-784 Korea

It is well known that SSCC (sulfide stress corrosion cracking) is caused by drastic ingression of hydrogen during the service and accumulation of hydrogen near the potential crack initiation site in the material. It is important to characterize the hydrogen trapping behavior to evaluate the service performance of the high strength pipeline steels.

In this study, the relationship between the hydrogen trapping behavior and SSCC susceptibility is evaluated in terms of alloy composition, microstructure and carbide behavior. The hydrogen trapping behavior was measured by electrochemical hydrogen permeation test cell (Devanathan cell). The SSCC susceptibility is evaluated by constant extension rate test and constant strain test method.

The hydrogen trapping behavior is affected greatly by microstructure and nature of carbide particles. The fine TiC, and NbC in the matrix of ferritic structure acts as strong irreversible trap sites whereas the bainitic structure acts as reversible trap site.

The SSCC susceptibility is closely related to not only the hydrogen trapping behavior but also the loading condition. As the activity of reversible trap site increases, SSCC susceptibility decreases under static loading condition below yield strength, whereas SSCC susceptibility increases under dynamic loading condition or above yield strength. As the activity of irreversible trap site increases, SSCC susceptibility increases regardless of loading condition. It is cased by the mixed effect of dislocation on hydrogen diffusion and trapping behavior.

Keywords : *SSCC, Devanathan cell, hydrogen permeation test, hydrogen trap, API grade steel*

1. Introduction

The API grade steels are required to have good mechanical property and high corrosion resistance; especially good resistance to hydrogen induced cracking (HIC) and sulfide stress corrosion cracking (SSCC). These two properties are the most important factors to evaluate the material property of the API grade steels. HIC and SSCC are generally induced by ingression of hydrogen during actual service because the hydrogen atoms are generated by metal corrosion and by improper cathodic protection.

To improve the mechanical property and corrosion resistance, the API grade steels are modified by addition of various alloying elements of Nb, V, Ti, Cr and Mo [1)-4)] and reduction of carbon content is also required to improve further the weldability.[5)] The thermomechanically controlled process (TMCP) is conducted to control the microstructure as well as to enhance precipitation of the fine carbide particles. The transport rate of hydrogen atoms in the steel directly affects the crack initiation and propagation, and consequently the susceptibility to HIC and SSCC. The effect of alloying element on the hydrogen transport has been studied by many investigators,[6)-8)] however, their results are still controversial and more studies are required for clarification. Especially, the corrosion failure induced by hydrogen ingression is believed to have a close relationship with permeation behavior of hydrogen atoms,[6)-8)] but the effects of alloying element on the diffusivity of hydrogen and on the susceptibility to SSCC have not been well investigated.

In this study, to investigate the relationship between the hydrogen trapping characteristics and SSCC susceptibility, 3 different steels of API-X60/65 grade are evaluated in terms of alloy composition, microstructure and carbide distribution. The diffusion process of hydrogen atoms and SSCC susceptibility are evaluated with respect to different loading conditions and the nature of trap sites. In order to understand the hydrogen trapping behavior, electrochemical hydrogen permeation test was conducted with successive 3 cycles of hydrogen charging and relaxation steps for each specimen. The SSCC susceptibility was evaluated by both constant extension rate test (CERT) and

constant strain test (CST) with different loading condition. In CST, the steel specimens are tested by two different strain conditions of 3.5% and 10% of fracture strain.

2. Expremental procedure

2.1 Specimen preparation

The steel specimens used in this investigation were API X60/65 grade steels which were produced by TMCP. The chemical compositions of the specimens are listed in Table. 1. A sheet metal having 12~16 mm thickness was machined to cylindrical tensile specimens with 25.4 mm gauge length and 6.35 mm diameter for SSRT and CST; and to coupon-type specimen with 2mm thickness, 48 mm diameter for hydrogen permeation test.

2.2 Electrochemical hydrogen permeation test

Hydrogen permeation test were conducted in an electrochemical dual cell called "Devanathan cell" as shown in Fig. 1.[9] The cell is composed of 2 compartments - the hydrogen generating cell (input side) and the hydrogen oxidizing cell (detection side) - separated by the coupon -like thin steel sample. The detection side was filled with 0.1M NaOH and applied with overvoltage of 50mV vs. OCP. The input side was filled with NACE (National Association of Corrosion Engineering) TM-01-77 solution and cathodic current of -2mA was applied galvanostatically. Before the test, all the specimens were mechanically polished with No. 1500 emery paper and chemically polished for 3 sec to eliminate air-formed oxide. To prevent the oxidation of specimen surface, thin Pd layer was electroplated on the oxidation side of specimen in the $PdCl_2$ 5g + NH_4OH 1L solution. The reference electrode was Ag/AgCl electrode and the counter electrode was Pt coil with the surface area of 2.2 cm^2. All the potential in this paper was measured with standard Ag/AgCl reference electrode.

2.3 SSCC susceptibility test

CERT was conducted to measure the SSCC susceptibility of specimens with the strain rates of 5×10^{-5}~2×10^{-6}/sec, and CST was conducted at two different levels of strain; 10% (plastic range in stress-strain curve) and 3.5% (elastic range) of fracture strain. The schematic diagram of SSCC susceptibility test set is shown in Fig. 1. The test solution was NACE standard TM-01-77

Table 1. Chemical composition of API grade steel specimens(wt%)

Steel	C	Si	Mn	P	S	Nb	V	Ti	Mo	Ca	Al	N
A	0.062	0.19	1.43	0.01	0.002	**0.045**	**0.038**	-	**0.13**	0.003	0.03	0.005
B	0.045	0.16	0.88	0.007	0.001	**0.039**	-	-	-	0.002	0.03	0.005
C	0.064	0.21	1.38	0.009	0.001	**0.037**	**0.030**	**0.013**	-	0.001	0.02	0.005

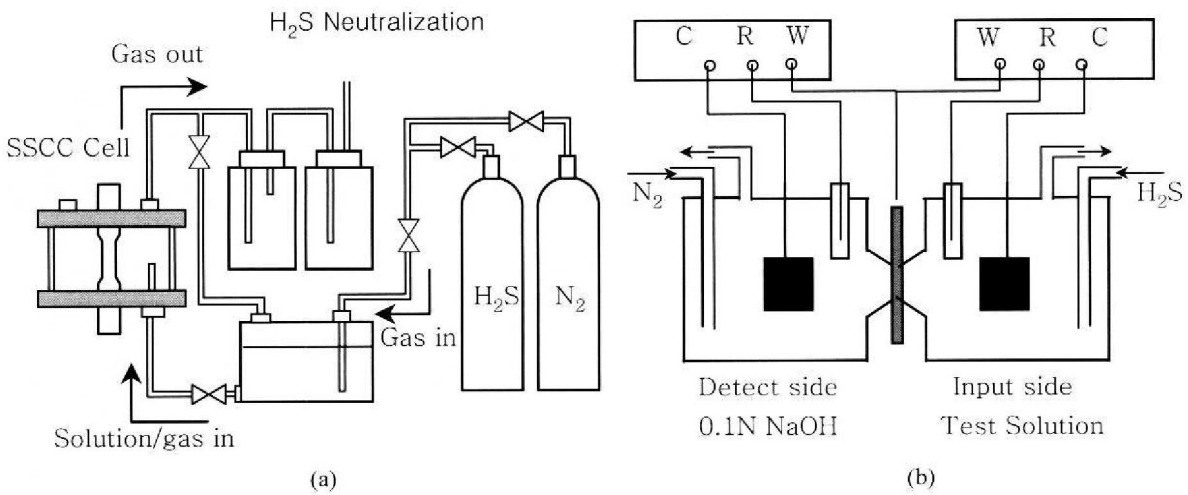

Fig. 1. Schematic diagram of experimental apparatus. CERT apparatus for measuring SSCC susceptibility Devanathan cell for electrochemical hydrogen permeation test

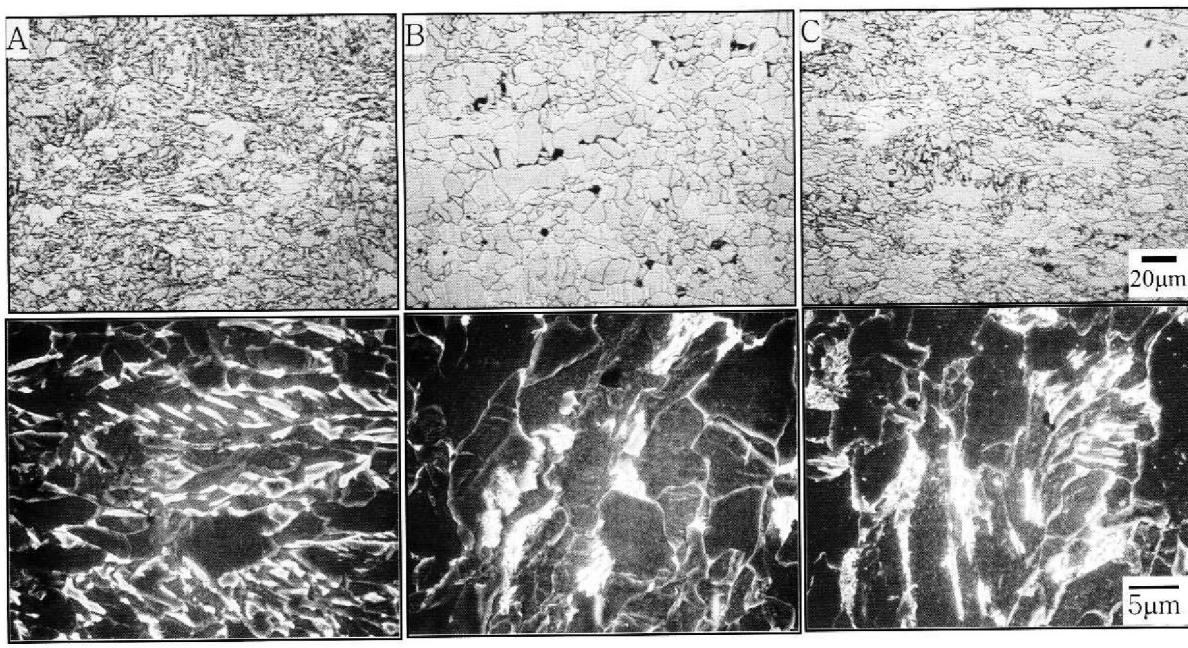

Fig. 2. Microstructures of specimens observed (a) by optical microscope in S-direction (X500, 2% nital etched), and (b) by SEM in L-direction (X2000)

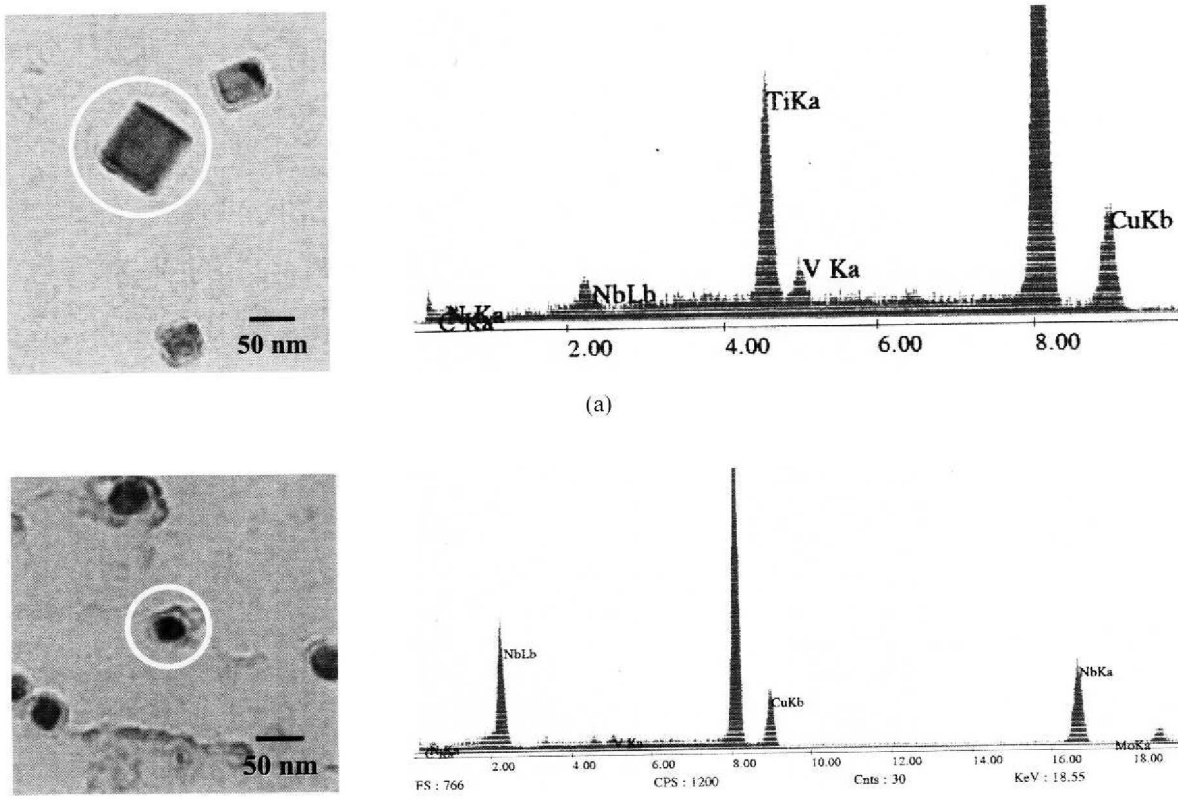

Fig. 3. (a) TEM image and EDX spectra on a typical cuboidal Ti(C,N) particle in Steel C (b) TEM image and EDX spectra on a typical spherical Nb(C,N) particle in Steel A, B, C.

solution (0.5% Acetic acid + 5% NaCl with saturated H_2S).

3. Results and discussion

3.1 Microstructures and TEM observation

Fig. 2 shows optical microstructures and SEM microstructures of the specimen cross-section normal to rolling direction. Steel A had mainly bainite structure with small fractions of pearlite and ferrite, whereas Steel B had typical ferrite structure with a small fraction of pearlite, and Steel C had ferrite structure with small fractions of pearlite and bainite islands. Depending on the amount and kind of alloying elements in the steel, various microstructures were developed during TMCP.

To characterize carbide distribution in the steel, TEM and EDX analyses were conducted on the replica of each specimen. Fig. 3 shows the TEM images and EDX spectra of typical carbide and nitride. Fig. 3(a) shows a cuboidal carbide observed from Steel C while Fig. 3(b) shows a spherical nitride observed from Steels A, B, C. Most of the carbides formed in Steels A and B were cuboidal NbC and NbVC. However, most of the carbides formed in Steel C were orthorhombic TiC along with small numbers of cuboidal NbC.

Table 2. The mean carbide particle size and carbide area ratio (area of carbide/area of matrix) for the steel specimens.

Specimes	Mean carbide particle size(nm)	Carbide area ratio
A	10.7	0.00526
B	10.3	0.00686
C	11.2	0.00899

Table 2 lists the mean carbide particle size and carbide area ratio (area of carbide/area of matrix) for the steel specimens. The mean carbide size in all 3 steels is quite similar, but the carbide area ratio of Steel A is relatively smaller than that of Steels B and C. The bainite structure observed from Steel A seems to be caused by the effect of Mo addition. Ravi et al.[4] have shown that Mo is present as solute atoms in the steel rather than as carbide precipitation, and thus Mo influences on the phase transformation and microstructure. Mo promotes the formation of bainite phase by suppressing the phase transformation from austenite to ferrite. Since carbon is used up for formation of bainite phase, the remained carbon content is not sufficient to make carbide. Therefore, the carbide content of Steel A is relatively smaller than that of Steels B and C.

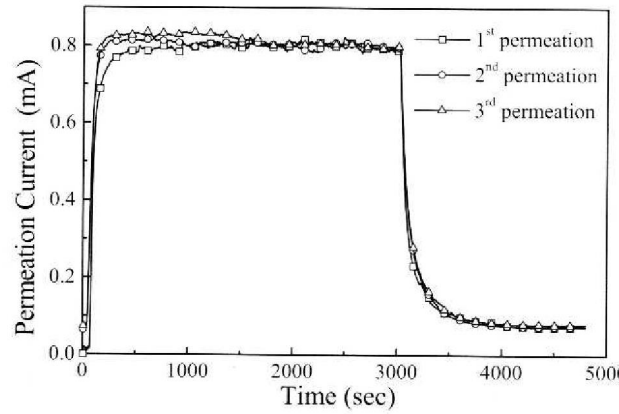

Fig. 4. Typical hydrogen permeation current transient in a steel specimen. (2 mA/cm^2, 3000sec galvanostatic control)

3.2 Hydrogen permeation test

Hydrogen permeation test was conducted using electrochemical method to characterize the hydrogen trapping behavior in the steel. Fig. 4 shows a typical result of hydrogen permeation test. The diffusivity was determined from the figure by both breakthrough time method, and relaxation time method. The relationships between the diffusivity and time for the respective test method are as follows.[10]

$$D_b = 0.76\frac{L^2}{\pi^2 t_b}, \qquad D_r = \frac{3\ln 3}{2t_r}\frac{L^2}{\pi^2}$$

The breakthrough time t_b and relaxation time t_r were measured from permeation curve. Specimen thickness L was measured both at the center and at the edge of each specimen after hydrogen permeation test.

During hydrogen permeation test, hydrogen atoms diffuse through the steel lattice. However, some of them may be trapped at impurities, which is called hydrogen trap site, such as carbide surface, dislocation, solute atom, void, and so on. Hydrogen trap sites are categorized as reversible trap and irreversible trap; The reversible site traps hydrogen atoms during the hydrogen charging step, but release them during rest potential step because of the smaller binding energy with hydrogen than thermal energy of hydrogen atom. But the irreversible trap sites whose binding energy with hydrogen is larger than the thermal energy of hydrogen atom trap hydrogen atoms before they are saturated with hydrogen atoms.

By 1000 sec (Fig. 3), the permeation current reached a steady-state which indicated all the trap sites in the specimen were saturated with hydrogen. The cathodic current was continuously imposed for 3000 seconds to

make sure that all the trap sites in the specimen were filled with hydrogen. During the rest potential step, the reversible trap site released hydrogen atoms to matrix because of high hydrogen concentration.

Both the reversible and irreversible trap sites are active during the 1st permeation, but only the reversible trap sites are active during 2nd and 3rd permeation. Therefore, the information about the reversible trap sites are accessible by analyzing 2nd(or 3rd) permeation current, and the information about irreversible trap sites are accessible by analyzing the difference between the 1st and 2nd permeation currents. The irreversible trapping coefficient is defined to determine the activity of irreversible trap sites. The relationship between the irreversible trapping parameter and diffusivities is as follows.

$$(irr.TP) = \frac{D_0}{D} - 1 = \frac{k}{p} N_T \qquad H + T \underset{p}{\overset{k}{\leftrightarrow}} H - T$$

D_0 is the diffusion coefficient of hydrogen through Fe lattice with no trap site, D is the hydrogen diffusivity in the steel with trap sites, k is forward reaction coefficient for hydrogen trapping reaction, p is reverse reaction coefficient for hydrogen trapping reaction, and N_T is trap density i.e. number of hydrogen atoms held by trap sites per volume of matrix.

3.3 Hydrogen trap site analysis

Fig. 5 shows the apparent diffusivity, lattice diffusivity, irreversible trapping parameter determined from the permeation curves presented in Fig. 4. The apparent diffusivity means the combined activity of both the reversible and irreversible trap sites, and the lattice diffusivity means only the activity of reversible trap sites because the irreversible trap sites were filled with hydrogen during 1st permeation. As the blocking effect of irreversible trap sites on the diffusion of hydrogen increased, the difference between the diffusivities measured from 1st and 2nd permeation curve decreased.

The effects of trap sites on the diffusivities of hydrogen and on the irreversible trapping parameter are well demonstrated in Fig. 5. It shows that Steel A has the lowest lattice diffusivity while Steel B has the highest apparent diffusivity and Steel C has the highest value of irreversible trapping parameter. In Steel A, the lattice diffusivity was the lowest although the amount of alloying elements was higher than the other 2 steels (Table 3). As explained previously in the analysis on the microstructure, it seems to be due to the effect of Mo on bainite transformation which suppresses carbide formation. The Mo present as solute atom in the steel acts as reversible trap sites. In

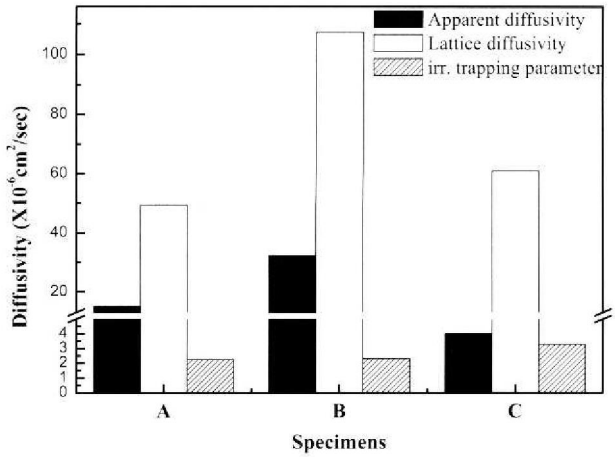

Fig. 5. Apparent diffusivity, lattice diffusivity, irreversible trapping parameter determined from permeation curves.

Table 3. Apparent diffusivity, lattice diffusivity, irreversible trapping parameter determined from permeation curves.

Measured parameters	Apparent diffusivity	Lattice diffusivity	Amount of Carbide former	Irreversible Trapping parameter
	X10^{-6}cm^2/sec		10^{-2}at%	
A	15.1	49.41	0.123	2.26
B	32.3	107.2	0.042	2.32
C	4.0	60.91	0.126	3.26

Steel B, both the apparent and lattice diffusivities are high because the blocking effect of hydrogen trap sites is small due to small amount of carbide forming elements. Steel C has a large amount of carbides and most of these carbides seem to act as irreversible trap site. Thus, Steel C has low apparent diffusivity and high lattice diffusivity and the highest value of the irreversible trapping parameter.

3.4 Constant extention rate test

To evaluate the SSCC susceptibility, CERT was performed with various strain rates. Fig. 6 shows the fracture time ratio which is defined as the ratio of fracture time tested in solution to that in air. In general, the fracture time ratio increases as the strain rate increases. It means that, with increasing the strain rate, the mechanical failure becomes dominant while the failure by SSCC becomes less dominant. However, the increment of the fracture time ratio of Steel A was smaller than those of the other 2 steels as the strain rate increased. It could be closely related to the hydrogen trap characteristics. As discussed previously, the hydrogen permeation test results suggested that the reversible trap sites in steel A was more active

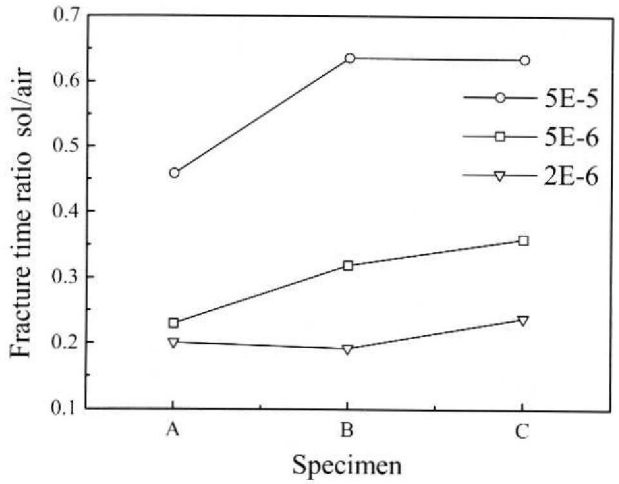

Fig. 6. The effect of the strain rate of CERT on the fracture time ratio.

than those in the other 2 steels. It means that the hydrogen transport is easier in Steel A due to fast dislocation movement at high deformation rate. Therefore, these hydrogen atoms moving along with dislocation can be rapidly trapped and accumulated at the fatal sites such as large inclusions which have high binding energy with hydrogen, and consequently cracks are developed at these fatal sites. This may explain the reason why the SSCC resistance decreases more in Steel A than in Steels B and C. Since the increment of the fracture time ratio of Steel C became relatively greater than those Steels A and B, the SSCC susceptibility of Steel C would be the largest among 3 steels.

3.5 Constant strain test

The CERT results showed that the SSCC susceptibility of steels depends on the loading condition. In order to understand clearly the effect of loading condition on the SSCC susceptibility, constant strain tests (CST) were conducted at 3.5% strain in elastic region of stress-strain curve and at 10% strain in plastic region. Fig. 7 shows the results of CST in a plot of time to fracture vs. applied load; (a) at 10% strain and (b) at 3.5% strain. At 10% strain the susceptibility of SSCC increased in the order of Steel C < Steel B < Steel A, which was equivalent to the CERT results. On the other hand, at 3.5% strain condition the susceptibility of SSCC increased in the order of Steel A < Steel B < Steel C.

In the elastic condition, the dislocation may be generated in the steel, but only little of them can move. On the other hand, in the plastic loading condition, the dislocations are generated and move rapidly through the

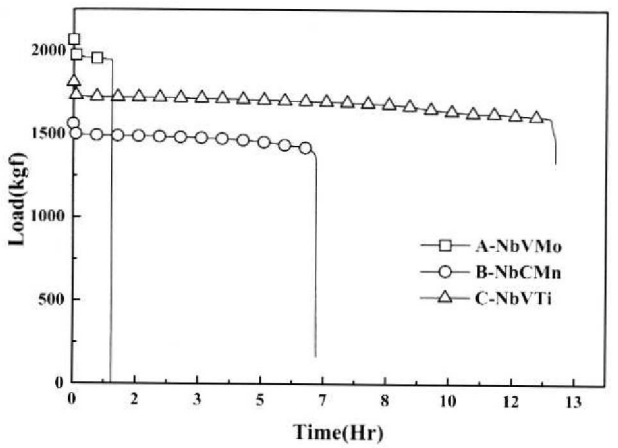

(a)

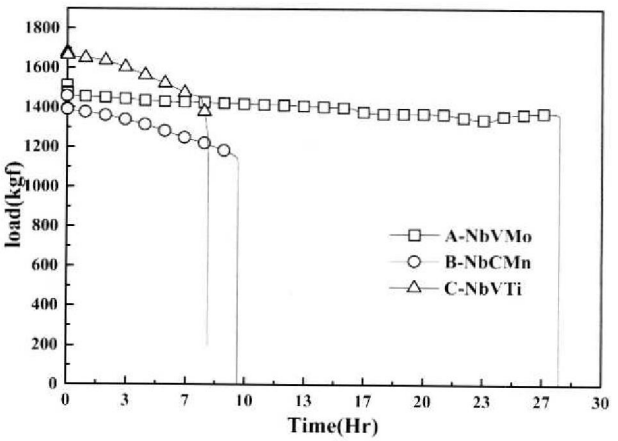

(b)

Fig. 7. Relaxation test results with stress level at 10% strain in plastic range (a), and with stress level of 3.5% strain in elastic range (b).

steel. At 10% strain condition, fast movement of dislocation transports the hydrogen atoms along with it. When the steel contains large amount of irreversible trap sites such as in Steel C, the moving hydrogen atoms along with dislocation will be trapped into the irreversible trap sites and the hydrogen atoms trapped already in the irreversible trap sites can not leave any more. Therefore, the diffusion of hydrogen is suppressed by the irreversible trap sites, and consequently the susceptibility to SSCC is reduced in the plastic loading condition. However, when the steel contains large amount of reversible trap sites such as in Steel A, the diffusion of hydrogen is highly assisted by moving dislocations and the cracks are developed easily at such high energy sites. Consequently the susceptibility to SSCC is accelerated in the plastic loading condition. Therefore, as shown in Fig. 7(a) under the plastic loading

condition, the susceptibility to SSCC is the highest for Steel A and the least for Steel C.

At 3.5% strain condition which is in elastic range of stress-strain curve, since the dislocations are continuously generated but do not propagate, the hydrogen transport assisted by propagating dislocation can not be taken into consideration. In this case, the activeness of the total hydrogen trap sites is the most important factor to determine the hydrogen diffusivity. As discussed previously, the total hydrogen trap sites are more in Steel A than in Steel C, and thus Steel A has lower susceptibility to SSCC than Steel C

3.6 Relationship between hydrogen trapping behavior & SSCC susceptibility

From the results of CERT and CST, it is observed that SSCC susceptibility depends upon the nature of the trap site and loading condition. Therefore, a great care should be required to interpret the relationship between the hydrogen trapping behavior and SSCC susceptibility.

The hydrogen diffusion is greatly affected by microstructure and nature of carbide particles. Steel A has bainite structure whereas Steels B and C have ferrite structure. The major portion of carbon in Steel A is used up for bainite phase formation while most carbons in Steel B and C form carbide particles. Therefore, the carbide area ratio and irreversible trapping parameter are greater in Steel C than in Steel A (Tables 2 and 3). It is interesting to compare between Steel A and B. Although the total amount of carbide former(Nb, V and Ti) is higher in Steel A than Steel B, the carbide area ratio and irreversible trapping parameter are less in Steel A than in Steel B because of high consumption of carbon during bainite transformation in Steel A. Therefore, the lattice diffusivity of Steel A was the lowest because the amount of alloying elements of Steel A was higher than those of the other 2 steels (Fig. 5). In Steel C, most carbides seemed to act as irreversible trap sites, and thus it had low apparent diffusivity, high lattice diffusivity and the highest value of the irreversible trapping parameter.

Among various carbide particles, it seems that TiC plays more active irreversible trap sites than both NbC and VC since Steel C has higher irreversible trapping parameter than Steel A, although Steel A contains higher amount of Nb and V than Steel C (Table 1 and 3). Depending on the nature of reversible or irreversible trap site, the diffusion of hydrogen is affected greatly by loading condition. As discussed previously for the results of CERT and CST (Figs. 6 and 7), in the plastic loading condition, the diffusion rate of hydrogen is reduced by the irreversible trap sites since they trap the hydrogen atoms moving along with dislocations and do not release the hydrogen atoms trapped already. Therefore, the irreversible trap sites such as TiC give beneficial effect on the improvement of SSCC resistance as observed from Steel C. For Steel A with large amount of reversible trap sites, in plastic loading condition, the diffusion rate of hydrogen is accelerated by supply of hydrogen atoms released from the reversible trap sites to moving dislocations. The hydrogen atoms moving along with dislocations are trapped at the inclusions or defect sites which have high binding energy with hydrogen, and the cracks are developed at such high energy sites. Therefore, high susceptibility can be observed from Steel A.

In elastic loading condition, the diffusion of hydrogen is affected by the amount of total trap sites, but not by dislocation movement. Steel A showed the best SSCC resistance as shown in Fig. 7(b) since the total hydrogen trap sites are higher in Steel A than in Steels B and C (Table 3).

4. Conclusion

1. The diffusion of hydrogen is affected greatly by micorstructure and nature of carbide particles. Steel A containing Mo has bainite structure while Steels B and C have mainly ferritic structure. Most carbides formed in Steels A and B are cuboidal NbC with small fraction of VC, and the carbides formed in Steel C are orthorhombic TiC with small fraction of NbC and VC. The average size of all the carbides is about 10 ㎛ regardless of their shape. The carbide area ratio is in the order of Steel A < Steel B < Steel C. The TiC plays more active irreversible trap sites than both NbC and VC since Steel C has higher irreversible trapping parameter than Steel A although Steel A contains higher amount of Nb and V than Steel C.

2. The SSCC susceptibility is closely related to the diffusion of hydrogen atoms, however, the diffusivity of hydrogen atoms depends largely on the loading condition. In the plastic loading condition, the diffusion rate of hydrogen in the steel containing irreversible trap sites such as TiC is reduced by the irreversible trap sites since they trap the hydrogen atoms moving along with dislocations, and thus the SSCC susceptibility is reduced. The diffusion rate of hydrogen in the steel containing reversible trap sites such as bainitic structure and atomic Mo is accelerated by supply of hydrogen atoms released from the reversible trap sites to moving dislocations, and thus the SSCC susceptibility is increased. In elastic loading condition, the diffusion of hydrogen is affected by the amount of total trap sites regardless of reversible or irreversible site, but not by dislocation movement.

References

1. J. C. Charbonnier, *Met. Trans. A* **16A**, 935 (1985).
2. T. Kaneko, Y. Okada, and A. Ikeda, *Corrosion*, **45**, 2 (1989).
3. B. D. Craig, *Corrosion*, **44**, 776 (1988).
4. K. Ravi, .Ramaswamy, and K. G. Namboodhiri, *Mat. Sci. & Eng.* **A169**, 111 (1993).
5. I. I. Valsilenko, O. Yu. Shul'te, and O. I. Radkevich, *Soviet Mat. Sci.*, **121**, 383 (1991).
6. R. A. Oriani, *Acta metall.* **18**, 147 (1970).
7. R. A. Oriani, J. P. Hirth, and M. Smialowski, "Hydrogen degradation of ferrous alloys", Noyes publication(1984)
8. G. M. Pressouyre and I. M. Bernstein, *Met. Trans. A* **9A**, 1571 (1978).
9. M. A. V. Devanathan and Z. Stachruski, *Proc. Royal Soc.* **A270**, 90 (1962).
10. N. Boes and H. Zuchner, *J. Less-comm. Met.* **49**, 223 (1976).